

HADRONIC CASCADE CALCULATIONS OF ANGULAR DISTRIBUTIONS OF INTEGRATED SECONDARY PARTICLE FLUXES FROM EXTERNAL TARGETS AND NEW EMPIRICAL FORMULAE DESCRIBING PARTICLE PRODUCTION IN PROTON-NUCLEUS COLLISIONS

J. RANFT† AND J. T. ROUTTI‡
CERN, Laboratory II, Geneva, Switzerland

Empirical formulae are described which represent the production of secondary pions and protons in high energy p -nucleus collisions; these have been introduced into hadronic cascade calculations. In addition, an empirical formula describing the production of low energy secondary protons and neutrons emitted by intranuclear cascade processes in hadron-nucleus collisions is proposed. By its use the intranuclear cascade particles can be introduced into computer programs calculating particle fluxes emerging from an external target hit by a high energy proton beam. The angular distributions calculated in this way are found to be in good agreement with experimental results obtained using activation detectors having different threshold energies.

1. INTRODUCTION

The intranuclear cascade initiated by the collision of high energy hadrons with nuclei was calculated by Bertini¹ and Barashenkov *et al.*² using the Monte Carlo method. Their methods enable one to calculate, among other quantities, the fluxes of protons and neutrons which are knocked out of the nuclei by the intranuclear cascade. A large number of such calculations has been reported and compared with experimental results.

Up to now these cascade particles were ignored in our extranuclear hadron cascade calculations,³ it being argued that for a well-developed cascade the total fluxes and other characteristics of the cascade are proportional to the high energy component. Good results were obtained with this assumption in most cases.

This assumption is not justified if the cascade is weakly developed as in the case of a proton beam hitting an external target or the ejection septum, etc. In such cases the fluxes of low energy cascade particles are certainly important at large angles and indeed large differences at angles larger than 30° were found in a comparison of measured integrated particle fluxes from external targets⁴ with particle fluxes obtained from the cascade calculations.

There are two reasons for this disagreement. The

production of high energy particles in the cascade calculations were represented by empirical Trilling type formulae which have a wrong transverse momentum dependence which differs from scaling behaviour. Therefore new empirical formulae with scaling behaviour and a better transverse momentum dependence have been introduced into the cascade calculations leading to an improved agreement but large differences at 90° from the target still exist. These formulae will be described in Sec. 2.

The second reason for the disagreement is that particles emitted by the intranuclear cascade were ignored. There are two possible ways of introducing the cascade protons and neutrons into extranuclear cascade calculations:

- (i) The Monte Carlo code calculating the intranuclear cascade might be used as a sub-routine each time a hadron-nucleus collision is considered in the extranuclear cascade code. This procedure has been used at Oak Ridge.⁵
- (ii) The fluxes of cascade particles might be represented by empirical formulae which are used to sample these particles each time a hadron-nucleus collision is considered in the extranuclear cascade calculation. This second procedure will be described here.

In the following discussion the centre-of-mass notation is used for high energy particle production (Sec. 2) and the laboratory frame for theoretical

† Visitor from Sektion Physik, Karl-Marx University, Leipzig, DDR.

‡ On leave of absence from Technical University of Helsinki, Otaniemi, Finland.

and experimental considerations of the intranuclear cascade particles (Secs. 3, 4 and 5).

2. EMPIRICAL FORMULAE DESCRIBING PARTICLE PRODUCTION IN p -NUCLEUS COLLISIONS WHICH ARE CONVENIENT FOR MONTE CARLO CALCULATIONS

During the past few years there has been much interest in particle production in hadron-hadron collisions. Experimental measurements, mainly for pp -collisions, were reported from all the larger accelerators. Theoretical efforts were concentrated on the development of models for multiparticle production and on the asymptotic behaviour of the production cross sections. Presently, the thermodynamic model⁶⁻¹⁰ describes practically all the data available at present accelerator energies and predicts the particle production at higher energies. Data on pion and proton production are explained equally well by the multi Regge-model.^{11,12}

The scaling conjecture of Feynman^{13,14} and the hypothesis of limiting fragmentation¹⁵ predict the asymptotic behaviour of cross sections. The discovery of Mueller¹⁶ that inclusive cross sections are related to discontinuities of elastic multiparticle scattering amplitudes, was the starting point for the applications of Regge phenomenology¹⁷ and dual models^{18,19} to inclusive multiparticle production. Most of these theoretical approaches were recently reviewed.²⁰

For Monte Carlo calculations of the hadronic cascade we need simple formulae, which permit the efficient selection of random secondary particle momenta and angles, describing the secondary particle spectra as well as possible. Empirical formulae, which represent known accelerator data,

and which behave at higher energies qualitatively as demonstrated by the theoretical models, cosmic ray and ISR results,²¹ are most useful for this task.

The formulae according to the thermodynamic model, which describe the data very well, are rather inconvenient for the random selection of particles.

In the past, the empirical formulae proposed by Cocconi, Koester and Perkins^{22,23} and Trilling²⁴ were used mostly in our cascade calculations³ but they have some shortcomings. At large angles or transverse momenta the proton and pion production, according to these formulae, drop much faster with increasing angle than the spectra according to the thermodynamic model which provides a good fit up to large transverse momenta. For improved cascade calculations it is more advantageous to describe particle production by empirical formulae having Feynman-scaling behaviour, which agree with the thermodynamic spectra. We use formulae similar to the ones described by Bali *et al.*²⁵ and Boggild *et al.*²⁶ The deviations from factorization between the longitudinal and transverse momentum distributions, which are known experimentally, are not important for Monte Carlo calculations of the hadronic cascade and are therefore omitted. Formulae with factorization are very convenient for Monte Carlo calculations because of the possibility to sample p_{\parallel} and p_{\perp} values independently. It is presently well known that there are deviations from scaling of the inclusive single particle spectra in the central region²¹ which can be understood naturally from the thermodynamic model.^{9,10} These deviations are not important for Monte Carlo calculations of the hadron cascade.

We define the formulae in the p - p centre-of-mass frame, using the longitudinal momentum p_{\parallel}^* and the transverse momentum p_{\perp} as variables together with the total centre-of-mass energy (of p - p), E_{CM} .

Pion production is described by

$$\frac{d^2N^*}{dp_{\parallel}^* dp_{\perp}} = \frac{U \exp(-A/E_{\text{CM}}^2 p^{*2}) p_{\perp} [\exp(-B p_{\perp}^2) + C \exp(-D p_{\perp})]}{(p_{\parallel}^{*2} + p_{\perp}^2 + m_{\pi}^2)^{1/2}}. \quad (1)$$

All momenta p and energies E are expressed in GeV/c and GeV, respectively. The parameters U , A , B , C and D were fitted to experimental data^{27,28} at 19.2 and 24 GeV/c and are given in Table I. $dN^*/dp_{\parallel}^* \cdot dp_{\perp}$ is measured in number of particles per (GeV/c)² and interaction. Secondary nucleon production is described by

$$\frac{d^2N^*}{dp_{\parallel}^* dp_{\perp}} = \frac{Q}{E_{\text{CM}}} \left(1 + \frac{V}{E_{\text{CM}}} p_{\parallel}^* + \frac{W}{E_{\text{CM}}^2} p_{\parallel}^{*2} \right) p_{\perp} [\exp(-B p_{\perp}^2) + C \exp(-D p_{\perp})] \quad (2)$$

The fitted values of the parameters Q , V , W , B , C and D are given in Table II.

Experimental data are only available for H_2 , Be, Al, Cu and Pb targets. Parameters for other target materials can be determined in most cases by

TABLE I
Parameters of the formula (1)

Particle	Target material	U	A	B	C	D
π^+	H_2	4.94	33.83	6.11	0.69	4.12
π^+	Be	1.81	33.39	3.01	5.12	7.34
π^+	Al	1.54	35.54	3.70	3.03	4.94
π^+	Cu	2.36	37.21	5.83	0.76	3.22
π^+	Pb	1.79	38.60	6.04	0.96	3.23
π^-	H_2	2.81	44.08	5.17	0.81	4.34
π^-	Be	1.52	42.74	5.33	0.82	3.53
π^-	Al	1.54	44.62	5.67	0.83	3.17
π^-	Cu	1.60	46.52	6.47	0.93	3.05
π^-	Pb	1.55	47.16	6.02	0.50	2.66

TABLE II
Parameters of formula (2) describing proton production

Target material	Q	V	W	B	C	D
H_2	8.71	0.86	-3.37	3.78	0.47	3.60
Be	2.65	1.03	-3.85	5.63	3.49	2.89
Al	2.76	-2.99	4.90	3.91	5.82	2.99
Cu	8.87	-1.78	0.30	5.38	0.38	1.41
Pb	3.10	1.01	-8.66	4.65	1.79	2.47

interpolation. It should, however, be noted that the experimental data^{27,28} are measured only for rather large secondary laboratory momenta. At these momenta the intranuclear cascade has mainly the effect of attenuating the particles created in primary nucleon-nucleus collisions. Particles created in secondary collisions are expected to modify strongly the spectra at lower momenta and large angles, and must be considered separately either by treating the intranuclear cascade or by representing the cascade protons and neutrons by a separate empirical formula as will be done in Sec. 3.

The multiplicities of pion production, according to formula (1), are obtained approximately

in the form

$$N_{\parallel \pm} = \left\{ 2U \left[E_1 \left(\frac{Am_{\perp}^2}{E_{CM}^2} \right) - E_1 \left(\frac{Ap_{CM,max}^2}{E_{CM}^2} \right) \right] + \frac{2UE_{CM}}{\sqrt{Am_{\perp}}} \operatorname{erf} \left(\frac{\sqrt{Am_{\perp}}}{E_{CM}} \right) \right\} \cdot \left\{ \frac{1}{2B} [1 - \exp(-Bp_{CM,max}^2)] + \frac{C}{D^2} [1 - (Dp_{CM,max} + 1) \exp(-Dp_{CM,max})] \right\} \quad (3)$$

where $m_{\perp} = \sqrt{m_{\pi}^2 + \langle p \rangle^2}$, and $E_1(x)$ and $\operatorname{erf}(x)$ are the exponential integral and the error function

$$E_1(x) = \int_x^{\infty} \frac{e^{-t}}{t} dt,$$

$$\operatorname{erf}(x) = \frac{2}{\pi} \int_0^x e^{-t^2} dt.$$

The second bracket in (3) can be approximated at larger values of $p_{CM,max}$, the maximum c.m.s. momentum, by

$$\left(\frac{1}{2B} + \frac{C}{D^2} \right).$$

We obtain the pion inelasticities

$$K_{\pi^{\pm}} = \frac{1}{E_{CM}} \int E_{\pi} \frac{d^2 N^*}{dp_{\parallel}^* dp_{\perp}} dp_{\parallel}^* dp_{\perp} \quad (4)$$

approximately in the form

$$K_{\pi^{\pm}} \approx \frac{2U}{\sqrt{A}} \operatorname{erf} \left(\frac{\sqrt{A} p_{CM,max}}{E_{CM}} \right) \left(\frac{1}{2B} + \frac{C}{D^2} \right). \quad (5)$$

For large $p_{CM,max}$, this becomes

$$K_{\pi^{\pm}} = \frac{2U}{\sqrt{A}} \left(\frac{1}{2B} + \frac{C}{D^2} \right). \quad (6)$$

The multiplicities and inelasticities of secondary protons are calculated from formula (2)

$$N_p = \frac{2Q}{E_{CM}} \left(p_{\parallel,max} + \frac{V}{2E_{CM}} p_{\parallel,max}^2 + \frac{W}{3E_{CM}^2} p_{\parallel,max}^3 \right) \cdot \left(\frac{1}{2B} + \frac{C}{D^2} \right), \quad (7)$$

$$K_p = \frac{2Q}{E_{CM}^2} \left(\frac{p_{\parallel,max}^2}{2} + \frac{V}{3E_{CM}} p_{\parallel,max}^3 + \frac{W}{4E_{CM}^2} p_{\parallel,max}^4 \right) \cdot \left(\frac{1}{2B} + \frac{C}{D^2} \right). \quad (8)$$

Numerical values of pion and proton multiplicities and inelasticities which were obtained using the parameters in Tables I and II are given in Table III. The inelasticities and multiplicities correspond approximately to those known experimentally.

TABLE III

Multiplicities N_i and inelasticities K_i of pions and protons calculated using the parameters in Tables I and II

$p_{0,\text{lab}}$ (GeV)	10		20		100		
	N_i	K_i	N_i	K_i	N_i	K_i	
p	H ₂	1.28	0.28	1.32	0.30	1.36	0.31
	Be	1.16	0.25	1.21	0.27	1.24	0.28
	Al	1.27	0.26	1.35	0.30	1.40	0.32
	Cu	1.21	0.22	1.37	0.26	1.46	0.28
	Pb	0.69	0.10	0.69	0.09	0.67	0.08
π^+	H ₂	2.46	0.19	3.10	0.19	4.17	0.19
	Be	1.62	0.13	2.05	0.13	3.14	0.13
	Al	1.79	0.14	2.27	0.14	3.51	0.14
	Cu	1.46	0.11	1.87	0.11	2.89	0.11
	Pb	1.23	0.09	1.57	0.09	2.45	0.09
π^-	H ₂	1.67	0.13	2.15	0.13	3.41	0.13
	Be	1.01	0.075	1.29	0.075	2.03	0.076
	Al	0.97	0.073	1.24	0.073	1.98	0.073
	Cu	0.94	0.073	1.24	0.073	2.01	0.073
	Pb	0.75	0.062	1.07	0.062	1.70	0.062

The pions multiplicities on H₂-targets are, however, somewhat too large. The numbers confirm the view, that at high secondary momenta, where the measurements^{27,28} were performed, the intranuclear cascade has mainly the effect of attenuating the particles created in forward direction and that the formulae (1) and (2) do not describe the particle spectra from nuclei at small momenta and large angles.

The formulae (1) and (2) are convenient for the random selection of secondary particle momenta (and angles after transforming) in hadronic cascade calculations and they were introduced into the corresponding computer programs.^{29,30}

3. EMPIRICAL FORMULAE DESCRIBING THE PRODUCTION OF CASCADE PROTONS AND NEUTRONS IN HADRON-NUCLEUS COLLISIONS

The formulae to be described are extracted from a large amount of published results of intranuclear

cascade calculations.^{1,2} The aim is not to represent all details of the fluxes of cascade protons and neutrons and no fit to the data is performed. For our purposes it is sufficient to represent the most important features of the data and their dependence on several parameters.

Some of these features are the following:

- (i) The number of cascade particles grows with the atomic weight of the target nucleus.
- (ii) The number of cascade particles grows initially with the kinetic energy of the projectile particles but becomes eventually constant for energies above about 5 GeV.
- (iii) Low energy particles are emitted more isotropically than high energy particles.
- (iv) There are slightly more neutrons than protons.
- (v) The average energies of cascade protons are slightly higher than the average energies of cascade neutrons.

The formulae are to be used for the Monte Carlo sampling of particles; therefore we give them in a form suitable for that purpose.

The distributions of intranuclear cascade particles are represented as functions of the following parameters:

- the kinetic energy of the projectile particle T_0 (in GeV) in the rest frame of the target nucleus, that is the laboratory frame,
- the kinetic energy of the emitted particle T (in GeV) in the rest frame of the target nucleus,
- the solid angle Ω (in radians)
- the production angle θ (in radians), and
- the atomic weight A of the target nucleus.

The double differential particle spectrum is written in a factorized form as

$$\frac{d^2N}{dTd\Omega} = f(A, T_0, T) g(A, T, \theta) \quad (9)$$

Here the function $g(A, T, \theta)$ is a normalized angular distribution which depends also on the kinetic energy of the produced particle. The function $f(A, T_0, T)$ gives the T dependence and does not depend on the production angle θ . It is normalized to the total multiplicity of emitted intranuclear cascade protons and neutrons.

The kinetic energy dependent function $f(A, T_0, T)$ is described by a superposition of two exponentials whose parameters are given separately for protons ($i = p$) and neutrons ($i = n$) and depend on T_0 and A as follows:

$$\left(\frac{dN}{dT}\right)_i = f_i(A, T_0, T) = \frac{n_{1i} \exp(-T/\alpha_{1i})}{\alpha_{1i}(1 - \exp(-T_0/\alpha_{1i}))} + \frac{n_{2i} \exp(-T/\alpha_{2i})}{\alpha_{2i}(1 - \exp(-T_0/\alpha_{2i}))}. \quad (10)$$

Here n_{1i} and n_{2i} are normalization parameters which are expressed as functions of A and T_0 (GeV) as follows:

$$\begin{aligned} n_{1p} &= \begin{cases} 0.03\sqrt{A} & \text{for } T_0 \leq 0.1 \\ 0.06\sqrt{A}(0.5 + (1 + \log_{10} T_0)^2) & 0.1 < T_0 < 5 \\ 0.20\sqrt{A} & T_0 \geq 5, \end{cases} & (11) \\ n_{2p} &= \begin{cases} 0.0035\sqrt{A} & \text{for } T_0 \leq 0.1 \\ 0.007\sqrt{A}(0.5 + (1 + \log_{10} T_0)^2) & 0.1 < T_0 < 5 \\ 0.024\sqrt{A} & T_0 \geq 5, \end{cases} \\ n_{1n} &= \begin{cases} 0.036\sqrt{A} & \text{for } T_0 \leq 0.1 \\ 0.06\sqrt{A}(0.6 + 1.3(1 + \log_{10} T_0)^2) & 0.1 < T_0 < 5 \\ 0.26\sqrt{A} & T_0 \geq 5, \end{cases} \\ n_{2n} &= \begin{cases} 0.0042\sqrt{A} & \text{for } T_0 \leq 0.1 \\ 0.007\sqrt{A}(0.6 + 1.3(1 + \log_{10} T_0)^2) & 0.1 < T_0 < 5 \\ 0.030\sqrt{A} & T_0 \geq 5. \end{cases} \end{aligned}$$

The total proton and neutron multiplicities are expressed as

$$\begin{aligned} \langle n_p \rangle &= n_{1p} + n_{2p}, \\ \langle n_n \rangle &= n_{1n} + n_{2n}. \end{aligned} \quad (12)$$

The parameters α_{1i} and α_{2i} also depend on T_0 and A as

$$\begin{aligned} \alpha_{1p} &= \begin{cases} (0.019 + 0.0017T_0)(1 - 0.001A) & \text{for } T_0 < 5 \\ 0.027(1 - 0.001A) & T_0 \geq 5, \end{cases} & (13) \\ \alpha_{2p} &= \begin{cases} (0.11 + 0.01T_0)(1 - 0.001A) & \text{for } T_0 < 5 \\ 0.16(1 - 0.001A) & T_0 \geq 5, \end{cases} \\ \alpha_{1n} &= \begin{cases} (0.017 + 0.0017T_0)(1 - 0.001A) & \text{for } T_0 < 5 \\ 0.026(1 - 0.001A) & T_0 \geq 5, \end{cases} \\ \alpha_{2n} &= \begin{cases} (0.1 + 0.01T_0)(1 - 0.001A) & \text{for } T_0 < 5 \\ 0.15(1 - 0.001A) & T_0 \geq 5. \end{cases} \end{aligned}$$

The average kinetic energy of one intranuclear cascade particle emitted is calculated from Eq. (10) to be

$$\begin{aligned} \langle T_i \rangle &= \int_0^{T_0} T \left(\frac{dN}{dT} \right)_i dT / \int_0^{T_0} \left(\frac{dN}{dT} \right)_i dT \\ &= \frac{n_{1i}}{n_{1i} + n_{2i}} \frac{\alpha_{1i} (1 - (1 + T_0/\alpha_{1i}) \exp(-T_0/\alpha_{1i}))}{1 - \exp(-T_0/\alpha_{1i})} \\ &\quad + \frac{n_{2i}}{n_{1i} + n_{2i}} \frac{\alpha_{2i} (1 - (1 + T_0/\alpha_{2i}) \exp(-T_0/\alpha_{2i}))}{1 - \exp(-T_0/\alpha_{2i})} \\ &\simeq 0.9 \langle T_{1i} \rangle + 0.1 \langle T_{2i} \rangle \end{aligned} \quad (14)$$

since, referring to Eq. (11), for all T_0

$$\frac{n_{1i}}{n_{1i} + n_{2i}} \simeq 0.9 \quad \text{and} \quad \frac{n_{2i}}{n_{1i} + n_{2i}} \simeq 0.1$$

The total energy spent in producing intranuclear cascade protons and neutrons is then equal to

$$T_{i,\text{tot}} = n_{1i} \langle T_{1i} \rangle + n_{2i} \langle T_{2i} \rangle. \quad (15)$$

The proton and neutron multiplicities $\langle n_p \rangle$ and $\langle n_n \rangle$ as expressed in Eqs. (11) and (12) are plotted in Fig. 1 for several materials as functions of the

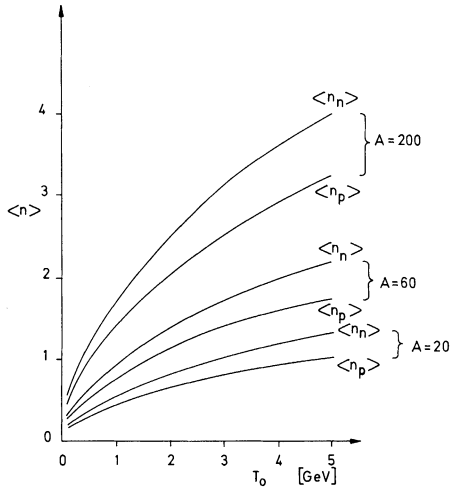


FIG. 1. Plot of the average number of intranuclear cascade protons and neutrons according to formula (12) as function of the kinetic energy T_0 for nuclei with atomic weights $A = 20, 60$ and 200 .

primary proton energy T_0 . The total energies $T_{i,\text{tot}}$ according to (15) are plotted in Fig. 2 as functions of the same variables.

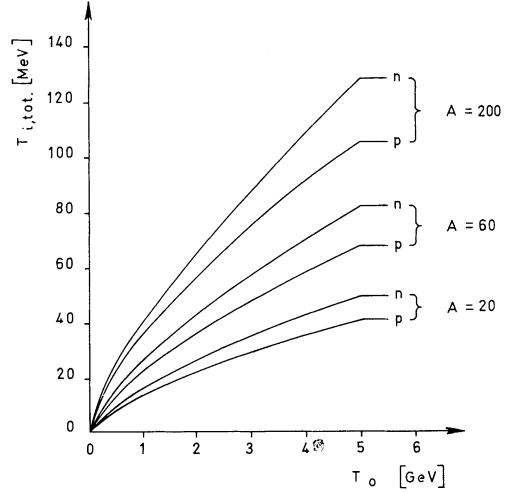


FIG. 2. Plot of the total kinetic energy spent for the production of intranuclear cascade protons and neutrons according to formula (15) as function of the kinetic energy T_0 for nuclei with atomic weights $A = 20, 60$ and 200 .

The angular distribution function $g(A, T, \theta)$ is represented by the formula

$$g(A, T, \theta) = \begin{cases} N \exp(-\theta^2/\lambda) & \text{for } 0 \leq \theta < \pi/2 \\ N \exp(-\pi^2/4\lambda) = \text{constant} & \pi/2 \leq \theta \leq \pi. \end{cases} \quad (16)$$

The parameter λ depends on the kinetic energy T of the produced particle and on the target material as

$$\lambda = (0.12 + 0.00036A)/T.$$

N is the normalization parameter normalizing the integrated angular distribution to unity.

4. HADRON CASCADE CALCULATIONS OF PARTICLE FLUXES FROM EXTERNAL TARGETS

The Monte Carlo method for hadron cascade computations described in Ref. 3 is used in program FLUKU²⁹ to calculate the fluxes of particles emitted from an external target hit by a high energy proton beam. These calculations are used to study the changes in inclusive single particle distributions, which are usually known only in the limit of very thin targets, due to the interactions of the particles in an external target.

The inclusive single particle distribution normalized to one interacting primary particle is a function of the primary momentum P_0 (GeV/c), the target material represented by the atomic weight A , the secondary momentum p (GeV/c) and the secondary particle angle θ (rad) in the laboratory frame.

$$\frac{d^2N}{dp d\Omega} = f_{p_0,A}(p, \theta). \quad (15)$$

In an external target of length l the interaction probability for an incoming particle is

$$\rho(l) = 1 - \exp(-l/\lambda_{\text{abs}}) \quad (16)$$

where λ_{abs} is the absorption length characteristic for the material and the incoming particle. Without secondary particle interactions in the target the flux from the target would be

$$F_{l,A,P_0}^0(p, \theta) = \rho(l)f_{p_0,A}(p, \theta). \quad (17)$$

Taking the effect of the cascade into account the single particle distribution from the target becomes

$$F_{l,r,A,P_0}(p, \theta) = D_{l,r,A,P_0}(p, \theta)F_{l,A,P_0}^0(p, \theta) \quad (18)$$

where r is the radius of the target. The function D expresses the relative change of the single particle distribution due to the cascade. For a thin target we expect $D = 1$. For extended targets we expect intuitively $D < 1$ for large secondary momenta p and small angles, since such secondary particles might only be absorbed inside the target and are not likely to be created in secondary particle collisions. We expect also $D > 1$ for small secondary momenta p and large angles since such particles are very likely to be produced in secondary particle interactions in the target.

The hadron cascade in the target is calculated with a Monte Carlo method. The functions F and F^0 calculated will be influenced by statistical errors as well as by uncertainties resulting from the approximations when sampling secondary particles. In the case of a thin target both functions have the same errors. Therefore we expect to obtain the quotient of both distributions

$$D_{l,r,A,P_0}(P, \theta) = \frac{F_{l,r,A,P_0}(p, \theta)}{F_{l,A,P_0}^0(p, \theta)} \quad (20)$$

with much smaller errors than either F or F^0 since most of the errors are expected to cancel.

The program FLUKU calculates in each run F , F^0 and D as functions of p and θ in the form of histograms. Furthermore we calculate the distributions which are obtained by integrating F and F^0 over the secondary particle angles

$$G_{l,A,P_0}^0(p, \theta_{\text{max}}) = 2\pi \int_0^{\theta_{\text{max}}} F_{l,A,P_0}^0(p, \theta) \sin \theta d\theta \quad (21)$$

$$G_{l,r,A,P_0}(p, \theta_{\text{max}}) = 2\pi \int_0^{\theta_{\text{max}}} F_{l,r,A,P_0}(p, \theta) \sin \theta d\theta \quad (22)$$

$$E_{l,r,A,P_0}(p, \theta_{\text{max}}) = \frac{G_{l,r,A,P_0}(p, \theta_{\text{max}})}{G_{l,A,P_0}^0(p, \theta_{\text{max}})} \quad (23)$$

and the distributions obtained by integrating F and F^0 over the secondary particle momenta starting from a given threshold P_{thr}

$$H_{l,A,P_0,P_{\text{thr}}}^0(\theta) = \int_{P_{\text{thr}}}^{P_0} F_{l,A,P_0}^0(p, \theta) dp \quad (24)$$

$$H_{l,r,A,P_0,P_{\text{thr}}}(\theta) = \int_{P_{\text{thr}}}^{P_0} F_{l,r,A,P_0}(p, \theta) dp \quad (25)$$

$$C_{l,r,A,P_0,P_{\text{thr}}}(\theta) = \frac{H_{l,r,A,P_0,P_{\text{thr}}}(\theta)}{H_{l,A,P_0,P_{\text{thr}}}^0(\theta)} \quad (26)$$

5. COMPARISON OF INTEGRATED ANGULAR DISTRIBUTIONS AROUND EXTERNAL TARGETS WITH EXPERIMENTAL DATA

Measurements with activation detectors of the hadron flux density around targets in external proton beams were reported in Ref. 4 and were compared with the results of the Monte Carlo hadron cascade program MAGTRA. This calculation used high-energy particle production according to Trilling type formulae which are unreliable at large transverse momenta and angles and also did not consider the intranuclear cascade protons and neutrons. The agreement was improved³¹ by replacing the Trilling type formulae by the formulae (1) and (2) but still the fluxes at 90° were very different indicating that the intranuclear cascade protons and neutrons dominate at large angles.

The empirical formulae describing the intranuclear cascade particle fluxes described in Sec. 3

have now been introduced into program FLUKU. Comparisons of the results of FLUKU with the measurements from Ref. 4 are presented in Fig. 3 and Fig. 4.

The measured particle fluxes⁴ at angles up to 60 degrees from a Cu-target hit by a 24 GeV/c

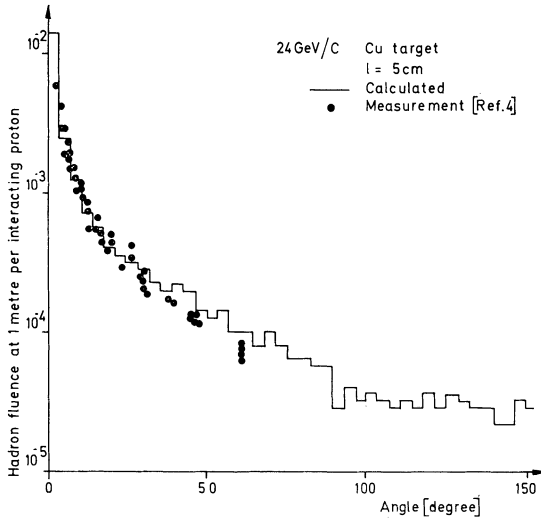


FIG. 3. Comparison of calculated and measured⁴ momentum integrated hadron fluxes around an external Cu target hit by a 24 GeV/c proton beam.

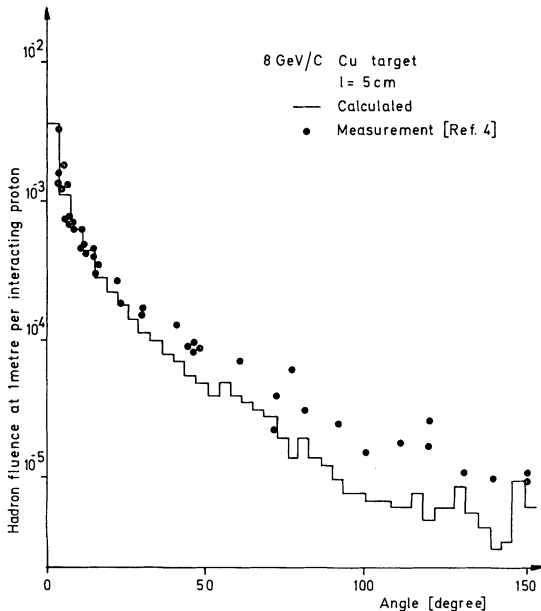


FIG. 4. Comparison of calculated and measured⁴ momentum integrated hadron fluxes around an external Cu target hit by an 8 GeV/c proton beam.

proton beam are compared in Fig. 3 with the calculated angular distributions around the target. The measured particle fluxes⁴ at angles up to 150° from a Cu-target hit by an 8 GeV/c proton beam are compared in Fig. 4 with the results of the calculation with FLUKU.

Figure 5 presents the comparison between the calculated and measured particle fluxes integrated above different threshold energies. The fluxes

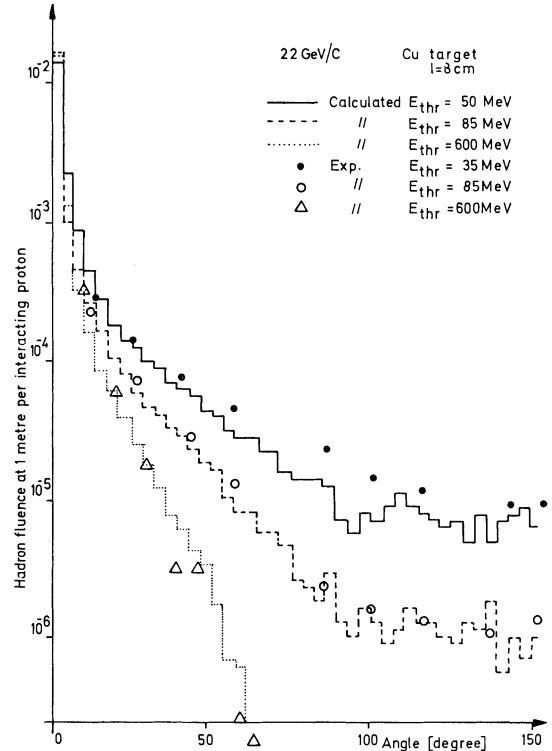


FIG. 5. Comparison of calculated and measured^{3,4} momentum integrated hadron fluxes around an external Cu target hit by a 22 GeV/c proton beam for three different threshold energies. $E = 50$ MeV is the lowest possible threshold energy in the calculation.

above 35 MeV and 85 MeV were measured up to 150° around a copper target of 1 mm diameter and 8 cm length bombarded by an external proton beam of 22 GeV/c momentum at the CERN Proton Synchrotron. Copper foils were placed at different radii around the target and the activities induced in the foils through spallation reactions by the secondary particles emerging from the target were studied after the exposure by using high-resolution gamma spectroscopy with Ge(Li)-detectors.^{3,2} A

multitude of spallation reactions were observed corresponding to different threshold energies, which are estimated by using the Rudstam formulae for the spallation reactions.³³ The results given for 35 and 85 MeV thresholds correspond to the reactions $\text{Cu}(p, \text{spall})^{56}\text{Co}$ and $\text{Cu}(p, \text{spall})^{46}\text{Sc}$, respectively. These and other results obtained in the experiment are described in detail elsewhere.³⁴ The third curve in Fig. 5 corresponds to a threshold energy of about 600 MeV of the reaction $\text{Hg}(p, \text{spall})^{149}\text{Tb}$. Angular distribution measurements around internal targets at the CERN Proton Synchrotron were performed with this high-sensitivity spallation detector during the CERN-LRL-RHEL shielding experiment.³⁵ Since this detector responds to very high energy particles only, the influence of vacuum chamber and other material around the target is not thought to be important and the comparison is made to the calculated fluxes resulting from interactions in the target alone.

We find a good agreement between the measured and calculated values in all cases considered. This includes both the shape and the absolute normalization of the angular distributions shown in Figs. 3 and 4. Experimental points given in Fig. 5 are normalized to the calculated curves at the smallest angles of the measurement, since the number of protons interacting in the target is not known. The shapes of the curves agree well for different threshold energies.

These comparisons might be taken as an indication that the formulae described in Sec. 2 describe adequately, at least for Cu-targets, the intranuclear cascade particle fluxes.

6. CONCLUSIONS

At high energies the total cross sections and the particle production for the purposes of the cascade calculations are sufficiently well known from the present accelerator and storage rings data up to the energies of about 1500 GeV. These data relate mostly to pp interactions but there are no qualitative differences expected in the energy-dependence of hadron-nucleon collisions. The particle production formulae described in Sec. 2 for high-energy p -nucleus collisions agree well with experimental data available from the present accelerators and storage rings, and can be used with confidence in

cascade calculations up to these energies. In the calculations the production of neutrons is treated in the same way as that of protons. This procedure is in accordance with all theoretical models on particle production and is supported also by experimental results at 24 GeV.³⁶ Some data are available for particle production in π -proton collisions and therefore it should be feasible to develop similar formulae as described here for π -nucleus collisions in the cascade calculations.

The formulae introduced in Sec. 3 to describe the low-energy intranuclear particles reproduce the angular distributions well when measured around external targets with integrating activation detectors. This agreement applies to the shape and the absolute normalization of the distributions, as well as to different threshold energies up to large angles. The inclusion of the intranuclear cascade particles into the calculation of extranuclear hadron cascades improves the accuracy of the results at large angles and in cases of weakly developed hadron cascades. The introduction of the formulae for intranuclear cascade particles into the calculations is done by using similar techniques as already employed in the production of high energy particles. Consequently this is done without significant increase of the complexity of the calculation.

ACKNOWLEDGEMENTS

The discussions with and suggestions by L. Hoffmann, K. Goebel and G. R. Stevenson of CERN, R. G. Alsmiller, Jr. of Oak Ridge National Laboratory, V. S. Barashenkov of JINR at Dubna, G. S. Levine of Brookhaven National Laboratory and R. H. Thomas of Lawrence Berkeley Laboratory are gratefully acknowledged. We are also indebted to W. H. Moore of Brookhaven National Laboratory for a careful reading of the manuscript.

REFERENCES

1. H. E. Bertini, *Proc. II Int. Conf. on Accelerator Dosimetry and Experience, Stanford, 1969*, p. 42, and Oak Ridge reports 1963-1971.
2. V. S. Barashenkov *et al.*, Dubna reports 1968-1971.
3. J. Ranft, *Particle Accelerators*, **3**, 129 (1972) and other papers quoted there.
4. G. S. Levine, D. M. Squier, G. B. Stapleton, G. R. Stevenson, K. Goebel and J. Ranft, *Particle Accelerators*, **3**, 91 (1972).

5. W. A. Coleman and T. W. Armstrong, Oak Ridge Report ORNL-4606 (1970) and other ORNL reports.
6. R. Hagedorn and J. Ranft, *Suppl. Nuovo Cimento*, **6**, 169 (1968).
7. J. Ranft, *Phys. Letters*, **31B**, 529 (1970).
8. H. Grote, R. Hagedorn and J. Ranft, *Particle Spectra*, CERN (1970).
9. R. Hagedorn and J. Ranft, to appear in *Nuclear Physics B* (1972).
10. Htun Than and J. Ranft, to be published in *Nuovo Cimento Letters* (1972).
11. L. Caneschi and A. Pignotti, *Phys. Rev. Letters*, **22**, 1219 (1969).
12. C. Risk and J. H. Friedman, *Phys. Rev. Letters*, **27**, 353 (1971).
13. R. P. Feynman, *Phys. Rev. Letters*, **23**, 1415 (1969).
14. R. P. Feynman, *Proc. 3rd Int. Conf. on High-Energy Collisions*, Stony Brook, N.Y., Sept. 1969.
15. J. Benecke, T. T. Chou, C. N. Yang and E. Yen, *Phys. Rev.*, **188**, 2159 (1969).
16. A. H. Mueller, *Phys. Rev.*, **D2**, 2963 (1970).
17. H. M. Chan, C. S. Hsue, C. Quigg and J. M. Wang, *Phys. Rev. Letters*, **26**, 672 (1971).
18. D. Gordon and G. Veneziano, MIT preprint (1970).
19. C. E. DeTar, K. Kang, C. I. Jan and J. H. Weiss, MIT preprint (1971).
20. G. Ranft and J. Ranft, *Fortsch. Phys.*, **19**, 393 (1971).
21. J. C. Sens, *Proc. IV Int. Conf. on High-Energy Collisions*, Oxford, April 1972.
22. G. Cocconi, L. J. Koester and D. H. Perkins, Lawrence Radiation Laboratory Report, UCRL-10022, p. 167 (1962).
23. G. Cocchini, preprint (1971), submitted to *Nucl. Phys.*
24. G. Trilling, Lawrence Radiation Laboratory Report UCID-10148 (1966).
25. N. F. Bali, L. S. Brown, R. D. Peccei and A. Pignotti, *Phys. Rev. Letters*, **25**, 557 (1970).
26. H. Bøggild, K. H. Hansen and M. Suk, Niels Bohr Institute preprint (1970).
27. J. V. Allaby, F. Binon, A. N. Diddens, P. Duteil, A. Klovning, R. Meunier, J. P. Peigneux, E. J. Sacharidis, K. Schlüpmann, M. Spighel, J. P. Stroot, A. M. Thorndike and A. M. Wetherell, Report CERN 70-12 (1970).
28. H. W. Wachsmuth and D. Heidt, personal communication (1971).
29. J. Ranft and J. T. Routti, Report CERN LABII-RA/72-8 (1972).
30. J. Ranft and J. T. Routti, to be published in *Computer Physics Communications*.
31. J. Ranft, Report CERN LABII-RA/71-3 (1971).
32. J. T. Routti and S. G. Prussin, *Nucl. Instr. Meth.*, **72**, 125 (1969).
33. G. Rudstam, *Z. Naturforschung*, **21a**, 1027, 1966.
34. J. T. Routti, in preparation.
35. W. S. Gilbert, D. Keefe, J. B. McCaslin, H. W. Patterson, A. R. Smith, L. D. Stephens, K. B. Shaw, G. R. Stevenson, R. H. Thomas, R. D. Fortune and K. Goebel, Lawrence Radiation Laboratory Report UCRL-17941 (1968).
36. J. Engler, W. Flauger, B. Gibbard, F. Mönning, K. Pack, K. Runge and H. Schopper, *Proc. IV Int. Conf. on High-Energy Collisions*, Oxford, April 1972.

Received 14 August 1972
and in revised form 10 October 1972